Published in Cell Calcium 37(3) : 233-243, 2005

Rapid turnover of the "functional" Na^+-Ca^{2+} Exchanger in Cardiac Myocytes Revealed by an Antisense Oligodeoxynucleotide Approach

Marcel Egger[1], Hartmut Porzig[2], Ernst Niggli[1], Beat Schwaller[3]

[1]University of Bern, Department of Physiology, Bühlplatz 5, CH-3012 Bern, Switzerland; [2]University of Bern, Department of Pharmacology, Friedbühlstrasse 49, CH-3010 Bern, Switzerland; [3]University of Fribourg, Division of Histology, Department of Medicine, 14, chemin du Musée, CH-1705 Fribourg, Switzerland

Running head: "functional half-life time" of the NCX

Key words: Sodium–calcium exchange, NCX, antisense oligodeoxynucleotides, cardiac myocyte, heart, intracellular calcium, calcium transport, caged calcium, Sf9 cells

Address for correspondence: Marcel Egger
Department of Physiology
University of Bern
Bühlplatz 5
CH-3012 Bern
Switzerland
Tel. ++41–31 631'87'37
FAX ++41–31 631'46'11
E-mail: egger@pyl.unibe.ch

ABSTRACT

Antisense oligodeoxynucleotides (AS-ODNs) were used in combination with transient functional expression of the cardiac Na^+-Ca^{2+} exchanger (NCX1) to correlate suppression of the Na^+-Ca^{2+} exchange function with down-regulation of NCX1 protein expression. In a *de-novo* expression system (Sf9 cells), a decrease in both, NCX1 mRNA and protein after AS-ODN application was paralleled by diminished NCX1 activity, a typical hallmark of an antisense effect. Although AS-ODN uptake was also efficient in rat neonatal cardiac myocytes, in whole-cell extracts of these cells treated with AS-ODNs, the amount of NCX1 protein determined in a quantitative binding assay remained almost unchanged, despite a prompt loss of NCX1 function. Immunocytochemical staining of myocytes revealed that most of the immunoreactivity was not localized in the plasma membrane, but in intracellular compartments and was barely affected by AS-ODN treatment. However, the small fraction of NCX1 located in the plasma membrane was significantly reduced. These results indicate that the "*functional half-life*" of the NCX1 protein in the plasma membrane of neonatal cardiac myocytes is surprisingly short, much shorter than reported *half-lifes* of about 30 h for other membrane proteins.

1. INTRODUCTION

The Na^+-Ca^{2+} exchanger (NCX) represents a transport protein that is expressed in the cell membrane of almost any cell type. In cardiac muscle cells, the activity of the NCX is particularly pronounced and the transporter is primarily responsible for the extrusion of Ca^{2+} from the cytosol during the relaxation of muscle force (for review see [1, 2]). The cardiac subtype NCX1 mediates countertransport of Na^+-and Ca^{2+} ions with a stoichiometry of 3:1, thus generating a membrane current (I_{NCX}) [3-5] (but see [6]). To date there are still considerable gaps in the understanding of the cellular and molecular function of the NCX1. This is, at least in part, due to the lack of a specific pharmacological inhibitor. The emerging knowledge about the cDNA encoding the cardiac NCX1 protein, which has been cloned and sequenced in 1990, enabled several studies using molecular biology techniques in order to overcome this limitation [7]. This includes site-directed mutagenesis [8-11], transgenic animals overexpressing NCX1 [12, 13], the generation of knock-out mice [14, 15], and in addition, antisense oligodeoxynucleotide (AS-ODN) strategies to block the *de-novo* synthesis of NCX in cell cultures [16-19]. The AS-ODN approach led to an almost complete functional suppression of NCX activity assessed by measuring I_{NCX} and by examining the Ca^{2+} transport using laser-scanning confocal imaging [16]. However, some discrepancies with regard to the protein stability and turnover of NCX1 in the cell membrane remain unsolved. The relatively quick decrease in I_{NCX}, which was substantial at 24 h and almost complete at 48 h in AS-ODN-treated neonatal cardiac cells indicated a comparably short half-life time ($t_{1/2}$) of less than 24 h [16]. In contrast, results from metabolic protein labeling studies suggested a $t_{1/2}$ of 33 h for NCX1 [20]. In principle, the action mediated by the AS-ODNs could be due to several mechanisms. The most obvious and expected one is the specific blocking and degradation of newly synthesized NCX1 mRNA. In addition, the antisense oligonucleotides

may have either a direct pharmacological effect on the NCX1 protein or unspecific toxic effects as previously shown in other systems [21-23].

To address the question of specificity of the antisense approach, two models (neonatal rat cardiac myocytes and insect Sf9 cells) and three methods (RT-PCR, immunohistochemistry and a quantitative binding assay) were combined, all of which are independent of the NCX1 function. The advantage of Sf9 cells is the lack of endogenous NCX1 protein and the ease at which these cells can be infected with baculovirus containing the cDNA for NCX1. In Sf9 cells expressing NCX1, the application of AS-ODNs resulted in a significant reduction of NCX1 mRNA, of the *de-novo* synthesis of the exchanger as evidenced by a quantitative binding assay and also by measuring the exchanger function. In contrast, in neonatal cardiac myocytes, we observed that in whole-cell homogenates the total amount of NCX1 epitopes recognized by the antibody was essentially unaltered after 48 h of AS-ODNs treatment, while the functionally active fraction of NCX1 in the sarcolemma had virtually disappeared. These observations provide a likely explanation for some of the discrepancies in previous reports on the functional or biochemical half-life of NCX1.

2. **METHODS**

2.1. Oligodeoxynucleotide uptake by rat cardiac myocytes and SF9 cells

Antisense oligodeoxynucleotides (AS-ODNs), nonsense (NS) and mismatch (MM) ODNs were identical to the ones described before [16]. The targeted sequence is part of the 3' untranslated region of the cardiac Na^{+}-Ca^{2+} exchanger (pos. 3065-3083, numbering according to the rat sequence) [24]. Phosphorothioate AS-ODNs (HPSF: High Purity Salt Free) were purchased from MWG Biotech (Ebersberg, Germany). In these ODNs, phosphorothioate groups replace four of the internucleotide phosphate groups at each end (5' and 3'), while all other linkages are normal phosphoester bonds. The modified "backbone" of such a mixed phosphorothioate oligo is resistant to the action of most exonucleases, but has a natural DNA center. Stock solutions of purified ODNs (100-300 μM) were stored at 4°C or for longer periods at -70°C. ODNs were added to the culture medium (3-5 μM final concentration for myocytes) for 24-48 h. Cultivated myocytes were then either fixed for immunohistochemistry or harvested for the binding assay experiments. To check for ODNs uptake, we used either AS-ODNs against the calcium-binding protein calretinin (CR) as described before or AS-ODNs against the NCX1, additionally labeled with FITC at the 3' end [25]. The CR AS-ODNs have the same length and approximately the same G/C content as the AS-ODNs directed against the NCX1 used for the experiments. For SF9 cells higher concentrations of ODNs (20-30 μM) were used to obtain comparable loading.

2.2. Neonatal rat cardiac myocytes

Primary cultures of neonatal rat cardiac myocytes from 2-3 day-old Wistar rats were prepared using established methods [26]. The After enzymatic dissoziation, myocytes were resuspened in medium M199 (Gibco) supplemented with 20 U/ml penicillin, 20 μg/ml

streptomycin and 10% FCS, then ODNs were added after 2 h at an initial concentration of 1 or 3 μM. Cultures were maintained in an incubator (1.5% CO_2) at 37°C for 24-48 h for experimental purposes. For binding experiments, myocytes were seeded in 25 cm^2 flasks at a density of 1-2 x 10^6 cells/ml and the AS-ODNs or NS-ODNs were added at an initial concentration of 1 or 3 μM after 2 h. After 48 h, cells were washed with PBS, scraped off the flask, transferred into a 10 ml tube and briefly centrifuged (3 min, 1000 rpm). The pelleted cells were resuspended in 5 ml of Dulbecco's Minimal Essential Medium (DMEM) supplemented with 5 % fetal calf serum (to block unspecific binding sites) and 0.1 % saponin (to permeabilize spontaneously forming membrane vesicles). This stock suspension was finally homogenized in a Potter-type glass-teflon homogenizer and used for the binding assay.

2.3. Quantification of NCX mRNA by RT-PCR

To quantify NCX1 mRNA levels in ODNs-treated cells (Sf9 or cultured neonatal myocytes), semi-quantitative RT-PCR with isolated total RNA was carried out. For first strand synthesis, 5 μg of total RNA was reverse-transcribed using random primers and reagents (RevertAid™ H^- First Strand cDNA Synthesis Kit, MBI Fermentas, Lab Force, Nunningen, Switzerland). Three different PCR reactions were carried out from the same batch (20 μl) of RT product isolated from Sf9 cells (2 μl RT product per PCR). The first reaction was aimed at amplifying part of the coding region (446–716) of the human NCX1 mRNA yielding a fragment of 271 base pairs (bp). The second PCR reaction used primers that amplify a fragment of 232 base pair centered around the annealing site of the AS-ODN in the 3'UTR region of the NCX1 mRNA. Forward primer: ATCCTGCCTCTTTGTGCTCCTATGGCTC; reverse primer: TACTTCGGCCCTAGTACAGAGTATGCTC. For the normalization of the RT-PCR reaction, amplification of Sf9 60S acidic ribosomal protein P2 (60S RP) mRNA with primers 60SP2-5' (AGACGTAGAGAAGATCCTCAGCTCTGTTGG) and 60SP2-3'

(TTGGTCTCCTTCTCTTCCTTCTTCTCCTCG) resulting in a band of 222 bp was carried out. All PCR programs consisted of an initial denaturing step (2 min, 94°C) followed by cycles of denaturing (20 s, 94°C), annealing at specific temperatures (40 s) and extension (40 s, 72°C). The annealing temperatures were optimized for each primer set and were 63°C for NCX/C (coding), NCX/3'UTR), rat NCX, 60S RP and 60°C for rat GAPDH. The optimal number of PCR cycles (midpoint of logarithmic range) was found to be 25 cyles. Equal aliquots of either NCX/C or NCX/3'UTR and 60S RP PCR product for Sf9 cell extracts and the previously described reactions for rat NCX and GAPDH were separated on a 2% agarose gel [27]. Images were acquired with a CCD camera and quantitatively analyzed using the BioRad software. For Sf9 samples the ratio NCX/60S RP and for neonatal rat myocytes the ratio NCX/GAPDH was calculated and the values for NS-ODNs treated samples were defined as 100%.

2.4. Protein binding assays

Binding experiments were carried out with the ^{3}H-labeled high-affinity monoclonal antibody R3F1 in order to quantify the expression of the NCX1 exchanger protein present in whole cell lysates of neonate myocytes as described in detail previously or in NCX1 baculovirus-infected Sf9 cells [28]. The results are expressed as the number of counts representing the specifically-bound radiolabeled NCX1 antibody R3F1 per μg of protein of whole-cell homogenate after subtraction of unspecific binding in the presence of a 50- to 100-fold excess of non-labeled R3F1. The protein concentrations in the lysates were quantified using the Micro BCA Protein Assay (Pierce, Rockford, IL) according to the protocol supplied by the manufacturer.

2.5. Immunofluorescence studies

Neonatal rat cardiac myocytes were washed with CMF-PBS and fixed with methanol at -20°C for 7 min. After washing with TBS (6 x 5 min, RT), the cells were incubated with the first antibody against the rat cardiac NCX1 (mAb R3F1, mouse monoclonal antibody) [28]. The monclonal antibody R3F1 was used at a dilution of 3.75 - 7.5 μg/ml in PBS + 10% bovine serum. After incubation overnight at RT, cells were washed with PBS (6 x 5 min) and incubated with the second antibody for 4 h in the dark. As second antibody, we used FITC-conjugated goat anti-mouse IgG (Fcγ-specific, Jackson Immunoresearch, West Grove PA) at a dilution of 1:100. Cells were washed once more as above and were visualized either on a Zeiss Axiovert (mag. 25 x) with the FITC-specific filters or on laser confocal microscopes (Zeiss, LSM 510).

2.6. Expression of the Na^+/Ca^{2+} exchanger and AS-ODN uptake

The human NCX1 was cloned and expressed in HEK293 cells, the cDNA being then subcloned into Baculovirus for expression in Sf9 cells [29]. Expression of NCX1 in Sf9 cells from *Spodoptera frugiperda* was described in detail recently [30]. For expression of NCX1 and AS-ODN uptake, Sf9 cells at a density of 1-2 x 10^6 cells/ml of serum free Grace's medium were transferred from the suspension culture to 25 cm^2 culture flasks, wherein they were permitted to attach for 40-60 min at 27°C. The supernatant was then replaced with fresh complete Grace's medium and ODNs were added after 24 h at an initial concentration of 20 μM (70% confluent monolayer), in the absence or presence of 10 μg/ml DOTAP (Roche Diagnostics, Switzerland). After incubation overnight, Sf9 cells were infected with MOI=5-10 from a recombinant baculoviral stock (0.5-1 x 10^8 pfu/ml; viral titer determined by end-point dilution). The culture flasks were maintained at 27°C in an incubator.

2.7. Functional tests of NCX1

The superfusion solution for functional tests of NCX1 contained (in mM): NaCl 140, KCl 5, $CaCl_2$ 1.8, $MgCl_2$ 1, HEPES 10, glucose 10. The pH was adjusted to 7.4 with NaOH. Extracellular solutions were changed with a half-time ($t_{1/2}$) of less than 0.5 s using a rapid switching system. Li^+ was used as a substitute for Na^+ in $[Na^+]_o$-free solutions. The pipette filling solution contained (in mM): Cs-aspartate 120, NaCl 10, K-ATP 5, Tetraethylammonium-Cl 20, HEPES 10, K_5-fluo-3 0.1 (Molecular Probes, Eugene, OR, USA), Na_4-DM-nitrophen 2, reduced glutathione (GSH) 2 and $CaCl_2$ 0.5 (pH 7.2, CsOH). Cells were loaded for at least 5 min by dialysis. For the functional NCX1 tests, Sf9 cells were infected with MOI=1. All experiments were carried out at ambient temperature (20°-22°C).

Flash-photolysis, I_{NCX} and Ca^{2+} measurements were described in detail elsewhere [31]. In brief, the I_{NCX} was recorded in the whole-cell configuration of the patch-clamp technique and the light from a xenon short-arc flash lamp (Strobex 238/278, Chadwick-Helmuth, El Monte, CA, USA, 230 Ws, pulse duration ≈1 ms) was used to photolyze intracellular DM-nitrophen in an epi-illumination arrangement on the confocal microscope (MRC1000; Biorad, Glattbrugg, Switzerland). During loading with DM-nitrophen and between flashes, cells were held at a membrane potential of -70 mV without correction for the junction potential. The membrane potential was depolarized to –40 mV 3 s prior to the flash. Data were analyzed using Igor Pro software (WaveMetrics, Lake Oswego, OR, USA). For Ca^{2+} time–course measurements, cells cultures were loaded with fluo-3 AM (3-5 μM for 30-45 min at 30 ºC). In addition, to obtain the Ca^{2+} concentrations with a high temporal resolution rapid line-scans were performed (up to 500 Hz). $[Ca^{2+}]_i$ was calculated according to the self-ratio method assuming a resting $[Ca^{2+}]_i$ of 100 nM and a K_d of fluo-3 for Ca^{2+} of 400 nM. All values were expressed as means ± S.E.M. Student's paired *t*-tests were used to test for significance. Significance is given as $P<0.05$ or <0.01, as indicated in the figure legends.

3. RESULTS

3.1. AS-ODNs uptake, NCX1 immunofluorescence and NCX1 binding studies with myocytes

Uptake of the AS-ODN was tested with fluorescently labeled ODNs as shown before [25]. Neonatal rat cardiac myocytes and SF9 cells were incubated with 3 μM or 30 μM FITC-labeled ODNs, respectively, for 48 h, which resulted in a marked intracellular fluorescence that was distributed throughout the cytoplasm, with a strong accumulation in perinuclear regions (Fig. 1A a,b). For the detection of the cardiac NCX1 protein the monoclonal antibody mAb R3F1, which recognizes epitopes present at the intracellular domain of the NCX1, was used (Fig. 1B) [28]. Cells were incubated with AS-ODNs (3 μM) for 48 h and compared to NS-ODNs (3 μM) treated myocytes. In control and AS-ODNs treated myocytes immunofluorescence was detected in the perinuclear space. However, the two cell populations differed with respect to the membrane-associated immunoreactivity. In about 60% of NS-ODNs-treated rat cardiac myocytes maxima of fluorescence could be observed in the plasma membrane (Fig. 1Ba), whereas only about 14% of NS-ODNs-treated myocytes showed membrane-associated immunoreactivity (Fig. 1Bb). Yet, no consistent differences in the overall intensities of the immunofluorescence between AS-ODNs treated cells or NS-ODNs treated cells were found. This is in contrast to the observation that under identical experimental conditions almost no NCX1 exchange function was detectable in AS-ODN-treated cells. Since “quantitative” immunofluorescence is of limited value for assessing protein expression levels, particularly in the case of membrane proteins, a protein-binding assay was carried out using the radiolabeled antibody R3F1 to measure cellular NCX1 levels. Initially, complete binding curves for AS-ODNs-treated and NS-ODNs-treated control cells were determined and were found to be almost identical (Fig. 1C). The plateau region of the binding curve (maximal specific binding) was reached at mAb concentrations >1 μg/ml. Therefore, a binding assay was carried out with a single free mAb concentration (1.5 μg/ml).

Analysis of 20 samples from 8 independent experiments revealed no significant differences between both groups (Fig. 1C, inset). From the immunocytochemistry results, it is evident that the majority of NCX1 molecules are localized in organelles (ER, Golgi, lysosomes) and only a small fraction of molecules is present in the plasma membrane. The lack of a difference in the number of antibody binding sites between AS- and NS-ODNs-treated cells despite a significant suppression of protein function is compatible with at least two possibilities: 1) A relatively small fraction of active exchangers in NS-ODNs-treated cells with a short functional half-life in the plasma membrane, that is absent or greatly diminished in AS-ODNs treated cells, might not be detectable in the large background of inactive NCX1 molecules present in the plasma membrane and other cellular locations; 2) AS-ODNs could promote a direct pharmacological inhibition of NCX1 without affecting protein synthesis. But this is highly unlikely because AS-, NS- and MM-ODNs all exhibited no toxic effects. To bypass the problems of high background levels of endogenous NCX1 molecules, and to address the above question, we decided to use the Sf9 cell system for the transient functional expression of NCX1. These cells have no endogenous NCX1, can be infected with baculovirus encoding the human NCX1 as described before and are thus ideally suited to investigate the effect of AS-ODNs on NCX1 biosynthesis directly [30].

3.2. Quantitative changes in Na^+-Ca^{2+} exchanger mRNA after AS-ODNs treatment

To investigate the specificity of the antisense approach, i. e. whether AS-ODNs indeed down-regulate NCX mRNA levels, semi-quantitative RT-PCR was carried out (Fig. 2A). For normalization of RT-PCR reactions from different RNA samples, mRNA for 60S RP (Sf9 cells) or GAPDH (myocytes) served as an internal standard. Each sample was analyzed twice independently (RT and PCR reactions). For all PCR reactions 25 cycles proved to be the optimal number (logarithmic phase). In non-infected Sf9 cells, no endogenous PCR product with the NCX/C primers was amplified confirming that primers are specific for human NCX1 (Fig. 2A,

CO 1–3). In infected and NS-ODN-treated Sf9 cells NCX1 signals were of variable intensities, but all larger than the ones in AS-ODNs treated cells (Fig. 2A), which on average reached only 30.6 ± 2.1% (mean ± SEM, n=6; $p < 0.01$) compared to NS-ODN-treated cells. A primer pair embracing the AS-ODN annealing site (NCX/3'UTR) gave very consistent results (Fig. 2A), 28.7 ± 10.1% ($p < 0.001$) compared to the NS-ODNs control. Thus, AS-ODNs treatment not only degrades the 3'UTR region of the NCX1 mRNA, i.e. their target region, but affect the coding region of NCX1 mRNA to a similar extent (approximately 70% reduction). AS-ODNs reduced mRNA levels in rat neonate myocytes to a lesser degree. We measured approximately 25% reduction in AS-ODNs-treated cells ($p < 0.05$ *vs*. NS-ODN, not shown).

3.2. Binding assay for the monoclonal antibody mAb R3F1 to SF9 cells expressing NCX1

Sf9 cells infected with NCX1 baculovirus (MOI=1, 48 h) were immunostained with the monoclonal antibody R3F1. Approximately 60% of Sf9 cells showed positive immunostaining. Staining intensities reflecting expression levels between individual Sf9 cells varied considerably. In all immunoreactive cells, the intracellular staining was present throughout the cytosolic space, though not homogenously distributed and hence, probably associated with intracellular compartments. Uninfected cells served as negative controls (Fig. 2B) and did not show specific immunostaining. For antibody binding experiments, Sf9 cells were infected with the NCX1 cDNA-containing baculovirus at two dilutions (MOI=1 or 5). Sf9 cells were first preloaded with ODNs (AS or NS) for 10–14 h. Then the cell cultures were infected with baculovirus and grown for an additional 48 h (in the presence of ODNs) before they were harvested for the binding assay. The specific R3F1 binding was assayed at 1.5-2 μg/ml radiolabeled mAb, i. e. in the plateau range of the binding curves determined previously (see Fig. 1C). Initial experiments with fluorescently labeled AS-ODNs (3 μM) revealed a significantly lower uptake of AS-ODNs in Sf9 cells as compared to neonatal rat myocytes and thus, higher AS-ODNs concentrations were

required (20-30 μM) to achieve comparable loading. Since AS-ODNs concentrations larger than 5 μM have been previously shown to induce nonspecific AS effects, functional assays in ODN-treated Sf9 cells were carried out (see below) indicating that these concentrations do not affect the viability of Sf9 cells. Under the condition of high multiplicity of infection with the baculovirus (MOI=5) NCX1 expression was reduced by approximately 30% in AS-ODN- treated (20 μM) cells as compared to NS-ODN (20 μM)-treated control cells (Fig. 2C). With the binding in NS-ODN-treated cells set to 100%, mAb binding in native (uninfected) Sf9 cells was less than 3 %, while binding in AS-ODNs treated cells was reduced to 71.7 ± 9.4 %. It is important to note that NS-ODN-treated cells rather than untreated NCX1-transfected Sf9 cells have to be taken as the corresponding controls, since in initial experiments we observed that the presence of polyanionic oligodeoxynucleotides had an effect on the rate of infection by the baculovirus (data not shown). By lowering the MOI to 1, the reduction in NCX1 binding induced by AS-ODNs was even more pronounced than at MOI of 5 (Fig. 2C). Under these conditions, an almost complete down-regulation of NCX1 expression was observed, in line with the RT-PCR results as expected for an AS-ODN effect. With the binding observed in NS-ODN-treated cells again set to 100%, the relative amount after AS-ODN treatment (18.1 ± 26.1 %, n=12) was almost identical to the values in uninfected control Sf9 cells (13.4 ± 13.3 %, n=3), both values being not significantly different from zero.

3.3. Blocking effects of AS-ODNs on NCX1 function

For functional studies, cultures of control Sf9 cells exposed to NS-ODNs (20 μM) and of those exposed to AS-ODNs (20 μM) were set up in parallel. For an initial examination of the NCX1 activity, the Na^+ concentration gradient across the sarcolemma of fluo-3 AM loaded cells was reversed by replacing extracellular Na^+ with Li^+. In the presence of extracellular Ca^{2+}, this maneuver induced Ca^{2+} entry into cells via NCX1 operating in the “reverse mode”. Because of

the exchange stoichiometry of 3 Na^+: 1 Ca^{2+}, an outward membrane current is generated in the Ca^{2+} influx mode, and an inward current is produced when Ca^{2+} moves in the outward direction. The activity of the exchanger in the reverse mode was estimated by determining the initial rate of rise in $[Ca^{2+}]_i$ ($d[Ca^{2+}]_i/dt$), measured as changes of fluo-3 fluorescence with confocal microscopy (Fig. 3). The Ca^{2+} entry and removal from the cytosol were almost exclusively due to the NCX1 activity as indicated by the almost complete absence of a detectable $[Ca^{2+}]_i$ decay when NCX1 was suppressed (see below) or in native Sf9 cells that show no basal NCX1 activity (data not shown). Figure 3A and B depict cell images and representative Ca^{2+} signals recorded from NCX1 expressing Sf9 cells after a 48h treatment with NS-ODNs (control) or from cells that had been exposed for the same time period to AS-ODNs. During the $[Na^+]_o$-free period, $[Ca^{2+}]_i$ rose by about 1.4 μM in control cells. Superfusion with $[Na^+]_o$ containing solution led to a monotonic decay of $[Ca^{2+}]_i$ to resting levels. In cells exposed to AS-ODNs (20 μM for 36 h), $[Ca^{2+}]_i$ rose to a significantly lower final level (190 nM). This was quantified by analyzing the Ca^{2+} transport ($d[Ca^{2+}]_i/dt$, Ca^{2+} influx, Fig. 3C). After 24 h of NCX1 expression, the NCX1-mediated Ca^{2+} influx in AS-ODN-treated Sf9 cells was reduced to about 34% of that in NS-ODN-treated cells. After 48 h of NCX1 expression $d[Ca^{2+}]_i/dt$ obtained in NS-ODNs was about 5-times larger than after 24 h, indicative of robust expression of the exchanger and incorporation of functional NCX molecules into the plasma membrane. On the other hand, the rate in AS-ODN-treated cells was only about 9% of that in NS-ODNs treated ones (Fig. 3C). In NS-ODNs treated cells, repeated application of $[Na^+]_o$ containing solution demonstrates that NCX1-mediated Ca^{2+} transport can be evoked several times (Fig. 3D). Interestingly, the second Ca^{2+} transient was reduced in amplitude, probably due to the reduced transmembrane concentration gradient for Na^+.

A specific test for the NCX function is the UV-flash photolysis approach to elevate $[Ca^{2+}]_i$ and then to follow the time-course of the $[Ca^{2+}]_i$ decay mediated by exchanger [27]. For these experiments, Sf9 cells were used and the data were obtained after 48 h of NCX1

expression. Intracellular Ca^{2+} concentration jumps were generated with UV-flash photolysis of caged Ca^{2+}. For this purpose, single cells were dialyzed with a pipette-filling solution containing 2 mM DM-nitrophen and 0.5 mM Ca^{2+} (in addition to the Ca^{2+} indicator fluo-3). Upon applying a flash of UV-light, $[Ca^{2+}]_i$ jumps of about 180 nM were induced (Fig. 4A and B). In NS-ODNs treated cells, $[Ca^{2+}]_i$ decayed to basal levels within 3 seconds (τ=470 ± 28.8 ms, Fig. 4A). This $[Ca^{2+}]_i$ step resulted in an I_{NCX} of 14.95 ± 2.9 pA (n=5). The control NS-ODNs did not significantly affect NCX1 function when compared to previous results obtained in the absence of ODNs. In cells exposed to AS-ODNs (Fig. 4B), a similar flash resulted in a comparable jump in $[Ca^{2+}]_i$, but the decay was significantly slower and, during the time of monitoring (approximately 1 min), did not reach basal $[Ca^{2+}]_i$. The initial Ca^{2+} transport rate ($d[Ca^{2+}]/dt$, Ca^{2+} efflux) in AS-ODN-treated cells was only 11% of that in NS-ODN-treated ones. The corresponding I_{NCX} was reduced to about 26% (Fig. 4C and D). The I_{NCX} was normalized to the cell membrane capacitance (7.35 ± 0.28 pF, n = 20) using cell geometry parameters (diameter: 15.38 ± 3.1 μm, n = 20) obtained from the confocal images. Although, probably additional Ca^{2+} transport systems working on slow time scale and contributing to the removal of Ca^{2+}, these findings suggest that the expression of NCX1 after AS-ODNs treatment was significantly diminished as evidenced by the reduced Ca^{2+} decay rate and the much smaller I_{NCX}.

4. DISCUSSION

In whole-cell extracts of neonatal rat cardiac myocytes treated with NCX1-specific AS-ODNs, the amount of immunoreactive exchanger protein remained almost unchanged despite efficient AS-ODN uptake and despite a prompt loss of NCX function. To explain this discrepancy, we combined 3 independent quantitative methods (RT-PCR, immunohisto-chemistry and a radioligand binding assay) for measuring NCX1 expression with functional tests based on flash-photolysis of caged Ca^{2+} and confocal imaging [28]. Our strategy also included AS-ODN suppression of de-novo protein expression in a background-free heterologous expression system. This approach involving several biophysical and an array of complementary molecular biology techniques has allowed us to derive novel conclusions regarding the NCX1 protein turnover in cardiac muscle cells.

4.1. "Mechanism" of antisense inhibition in neonatal myocytes and in Sf9 cells expressing NCX1

Interestingly, confocal images of R3F1 mAb-immunostained neonatal rat myocytes revealed that a large fraction of NCX1 immunoreactivity was localized to the plasma membrane and in cytoplasmic regions, with a high density in the perinuclear region, previously reported as "organized in reticular patterns" [32]. However, no striking differences in the intensity of overall staining were detected between AS- and NS-ODN-treated cultured myocytes. Since the NCX1 activity is mediated only by the subpopulation of exchanger molecules, which are both I) localized in the sarcolemma and II) functional, our results suggested that this fraction of NCX1 population is small compared to the amount of immunoreactive protein detected by the R3F1 antibody.

A way out of the dilemma was to investigate the effect of NCX1 AS-ODNs in Sf9 insect cells i.e. in a cellular system without native NCX1 activity, which would allow us to verify that the AS-ODN effect was caused by the degradation of NCX1 mRNA leading to decreased expression levels and subsequently reduced activity of NCX1 protein.

In order to effectively apply the antisense approach on NCX1-infected Sf9 cells, several points have to be considered. The first is the kinetics of infection, which depend on the multiplicity of infection (MOI) of the inoculum and, related to that, the delay until functionally active NCX1 molecules are expressed in the plasma membrane. Secondly, the kinetics of uptake of the ODNs have to be monitored, which depend on the extracellular ODN concentration and the type of reagents used to facilitate ODN uptake (e. g. lipofection reagents). We found that the uptake of fluorescently labeled ODNs in Sf9 cells was considerably less efficient than in neonatal cardiac myocytes, necessitating extracellular ODN concentrations of 30 μM (instead of 3 μM) for comparable intracellular fluorescence intensities. Using this AS-ODN loading protocol, RT-PCR amplification of either the region containing the AS-ODNs binding site or a region within the coding part of the NCX1 mRNA resulted consistently in a signal approximately 70% weaker in Sf9 cells treated with AS-ODNs than in NS-ODNs-treated cells. In the protein binding assay, the efficiency of the AS-ODNs to block the *de-novo* synthesis of NCX1 protein was clearly dependent on the MOI. At a MOI of five, NCX1 protein levels in AS-ONDs treated cells were ≈ 30 % lower than in NS-ODN-treated cells and at MOI of one, NCX1 protein levels determined after 48 h of AS-ODN-treatment ranged barely above the nonspecific background value obtained for uninfected Sf9 cells. Hence, at a low to moderate MOI the NCX1 synthesis can be almost completely blocked by AS-ODNs. Thus, RT-PCR and protein binding results fully support the notion that AS-ODNs efficiently suppress NCX1 expression. Effective suppression of NCX1 expression was also confirmed by two functional assays (1) testing the reverse mode of the NCX1 protein in the absence of external sodium and (2) measuring the forward mode by

rapidly increasing $[Ca^{2+}]_i$ by flash photolysis of caged Ca^{2+}. Both, Ca^{2+} efflux as well as Ca^{2+} influx were similarly reduced in AS-ODN-treated Sf9 cells. The almost complete blocking of NCX1 synthesis observed at both, mRNA and protein levels in AS-ODNs treated cells clearly parallels the reduced NCX1 function.

4.2. Rapid turnover of the "functional" NCX1

If we assume the same antisense mechanism, a reduction of the protein expression, also to be present in neonatal cardiac myocytes (as also evidenced by decreased mRNA levels), how can we reconcile the apparent paradox that NCX function is dramatically reduced after 48 h of AS-ODNs treatment, while the total amount of NCX1 measured in the binding assay is not significantly affected?

In neonatal cardiac myocytes NCX1 immunoreactivity (Fig. 1) resides in various organellar compartments most likely including SR, Golgi, vesicular compartments transporting the NCX1 protein to or from the plasma membrane and finally in the plasma membrane. Yet the only functionally relevant species is the small fraction of NCX1 protein located in the plasma membrane. This distribution of NCX1 is not surprising, since the endoplasmic reticulum has important functions as a quality-control system for newly synthesized proteins, so that only native conformers reach their final destinations such as the plasma membrane. Non-native conformers or misfolded proteins are either retained or degraded, respectively and apparently, a large fraction of ER-synthesized proteins fail to fold and mature properly (reviewed in [33]). Since NCX1 protein turnover has been determined in whole-cell lysates, the relatively long $t_{1/2}$ (33 h) is fully compatible with a model consisting of a rather short protein synthesis time and a rapid insertion into the plasma membrane, while a relative slow process accounts for membrane protein retrieval leading to either recycling or degradation of the NCX1 molecules. Such a model

is further supported by our observation of a distinct loss of membrane-associated immunoreactivity in AS-ODN-treated cardiac cells. Even among the population of NCX molecules present in the plasma membrane, only a fraction might be functionally active. This is in line with previous findings, where the effect of AS-ODNs on target protein levels was found to be smaller than the one calculated from the loss of functional activity [34]. Hence, the "functional" half-life of the NCX1 protein measured as exchange activity and the half-life determined by [^{35}S]methionine labeling may well have significantly different time scales. Additionally, a relative resistance of the antibody epitope against proteolytic cleavage during degradation might help to explain the discrepancy between the levels of NCX1 immunoreactivity and NCX1 function after AS-ODN treatment.

4.3. Comparison with previous studies

The half-life ($t_{1/2}$) of the NCX1 protein in neonatal cardiac cells was previously reported by different laboratories to range between 10-33 h, possibly depending on the methodology applied [16, 20]. Although the $t_{1/2}$ value found in our study is in line with previous reports on $t_{1/2}$ values of other membrane proteins, conclusions need to be drawn with some caution [35]. In most reports, cells are metabolically labeled with a pulse of ^{35}S[methionine] and then the time course of the disappearance of incorporated radioactivity in the molecules of interest is monitored by immunoprecipitation. Earlier studies have shown that several proteolytic fragments of the exchanger observed in Western blots of NCX1 protein preparations retained immunoreactivity towards antibodies, such as R3F1, with epitopes within the intracellular hydrophilic loop [36, 37]. All evidence obtained previously suggests that the *de-novo* synthesis in neonate cardiac myocytes is fast and the functional half-life of NCX1 in the plasma membrane in these cells is short, which is compatible with an almost complete loss of activity 48 h after AS-ODNs treatment. Besides the putative mechanisms discussed above, the rather slow time

course of NCX1 protein rundown in the study of Slodzinski *et al*. 1998, may well be explained by the lower concentration of AS-ODNs used (0.5 μM *versus* 3 μM in the present study) [20]. On the other hand, Takahashi *et al*. 1999, using a concentration of 10 μM reported a decrease in the level of NCX1 expression in the order of 20% within 24h [38].

Our results indicate that by far the largest fraction of NCX1 immunoreactivity is not residing in the plasma membrane and that the functional NCX1 proteins have a very high turnover rate such that a blockage of protein synthesis is quickly translated to impaired NCX1 function. Whether this high turnover rate is specific for neonate cardiac myocytes and why this energetically unfavorable mechanism is maintained needs to be addressed in further experiments.

5. ACKNOWLEDGEMENTS

This work was supported by the Swiss National Science Foundation (31-68056.02 to ME, 31-61344.00 to E.N., 31-063448.00/1 to BS). We are grateful to D. Schulze, Baltimore, for the Baculovirus, D. Lüthi, Bern and M. Pfefferli, Fribourg for technical assistance.

6. REFERENCES

[1] M. Egger, E. Niggli. Regulatory function of Na-Ca exchange in the heart: milestones and outlook. J Membr Biol, 168 (1999) 107-130.

[2] M. Shigekawa, T. Iwamoto. Cardiac Na^+-Ca^{2+} exchange: molecular and pharmacological aspects. Circ Res, 88 (2001) 864-876.

[3] J.P. Reeves, C.C. Hale. The stoichiometry of the cardiac sodium-calcium exchange system. J Biol Chem, 259 (1984) 7733-7739.

[4] H. Dong, J. Dunn, J. Lytton. Stoichiometry of the Cardiac Na^+/Ca^{2+} exchanger NCX1.1 measured in transfected HEK cells. Biophys J, 82 (2002) 1943-1952.

[5] M. Hinata, H. Yamamura, L. Li, Y. Watanabe, T. Watano, Y. Imaizumi, J. Kimura. Stoichiometry of Na^+-Ca^{2+} exchange is 3:1 in guinea-pig ventricular myocytes. J Physiol, 545 (2002) 453-461.

[6] Y. Fujioka, M. Komeda, S. Matsuoka. Stoichiometry of Na^+-Ca^{2+} exchange in inside-out patches excised from guinea-pig ventricular myocytes. J Physiol, 523 (2000) 339-351.

[7] D.A. Nicoll, S. Longoni, K.D. Philipson. Molecular cloning and functional expression of the cardiac sarcolemmal Na^+-Ca^{2+} exchanger. Science, 250 (1990) 562-565.

[8] D.A. Nicoll, L.V. Hryshko, S. Matsuoka, J.S. Frank, K.D. Philipson. Mutation of amino acid residues in the putative transmembrane segments of the cardiac sarcolemmal Na^+-Ca^{2+} exchanger. J Biol Chem, 271 (1996) 13385-13391.

[9] A.E. Doering, D.A. Nicoll, Y. Lu, L. Lu, J.N. Weiss, K.D. Philipson. Topology of a functionally important region of the cardiac Na^+/Ca^{2+} exchanger. J Biol Chem, 273 (1998) 778-783.

[10] D.A. Nicoll, M. Ottolia, L. Lu, Y. Lu, K.D. Philipson. A new topological model of the cardiac sarcolemmal Na^+-Ca^{2+} exchanger. J Biol Chem, 274 (1999) 910-917.

[11] T. Iwamoto, A. Uehara, I. Imanaga, M. Shigekawa. The Na^+/Ca^{2+} exchanger NCX1 has oppositely oriented reentrant loop domains that contain conserved aspartic acids whose mutation alters its apparent Ca^{2+} affinity. J Biol Chem, 275 (2000) 38571-38580.

[12] S. Adachi-Akahane, L. Lu, Z. Li, J.S. Frank, K.D. Philipson, M. Morad. Calcium signaling in transgenic mice overexpressing cardiac Na^+-Ca^{2+} exchanger. J Gen Physiol, 109 (1997) 717-729.

[13] C.M. Terracciano, K.D. Philipson, K.T. MacLeod. Overexpression of the Na^+/Ca^{2+} exchanger and inhibition of the sarcoplasmic reticulum Ca^{2+}-ATPase in ventricular myocytes from transgenic mice. Cardiovasc Res, 49 (2001) 38-47.

[14] H. Reuter, S.A. Henderson, T. Han, T. Matsuda, A. Baba, R.S. Ross, J.I. Goldhaber, K.D. Philipson. Knockout mice for pharmacological screening: testing the specificity of Na^+-Ca^{2+} exchange inhibitors. Circ Res, 91 (2002) 90-92.

[15] K.D. Philipson, S. Henderson, M. Jordan, K. Roos, J. Goldhaber, C. Motter, T. Han, J. Frank, R. Roos, D. Nicoll, M. Ritter, M. Friedlander. Functional adult myocardium in the absense os sodium-calcium exchanger: Specific knockout of NCX1. Biophys J, 86 (2004) 224a.

[16] P. Lipp, B. Schwaller, E. Niggli. Specific inhibition of Na-Ca exchange function by antisense oligodeoxynucleotides. FEBS Lett, 364 (1995) 198-202.

[17] K. Takahashi, K.S. Bland, S. Islam, M.L. Michaelis. Effects of antisense oligonucleotides to the cardiac Na^+/Ca^{2+} exchanger on cultured cardiac myocytes. Biochem Biophys Res Commun, 212 (1995) 524-530.

[18] M.K. Slodzinski, M.P. Blaustein. Physiological effects of Na^+/Ca^{2+} exchanger knockdown by antisense oligodeoxynucleotides in arterial myocytes. Am J Physiol, 275 (1998) C251-259.

[19] B.N. Eigel, R.W. Hadley. Antisense inhibition of Na^+/Ca^{2+} exchange during anoxia/reoxygenation in ventricular myocytes. Am J Physiol Heart Circ Physiol, 281 (2001) H2184-2190.

[20] M.K. Slodzinski, M.P. Blaustein. Na^+-Ca^{2+} exchange in neonatal rat heart cells: antisense inhibition and protein half-life. Am J Physiol, 275 (1998) C459-467.

[21] C.A. Stein, R. Narayanan. Antisense oligodeoxynucleotides. Curr Opin Oncol, 6 (1994) 587-594.

[22] A.D. Branch. A good antisense molecule is hard to find. Trends Biochem Sci, 23 (1998) 45-50.

[23] I. Lebedeva, C.A. Stein. Antisense oligonucleotides: promise and reality. Annu Rev Pharmacol Toxicol, 41 (2001) 403-419.

[24] W. Low, J. Kasir, H. Rahamimoff. Cloning of the rat heart Na^+-Ca^{2+} exchanger and its functional expression in HeLa cells. FEBS Lett, 316 (1993) 63-67.

[25] B. Schwaller, M. Egger, P. Lipp, E. Niggli. Application of antisense oligodeoxynucleotides for suppression of Na^+/Ca^{2+} exchange. Methods Enzymol, 314 (2000) 454-476.

[26] S. Rohr. A computerized device for long-term measurements of the contraction frequency of cultured rat heart cells under stable incubating conditions. Pflugers Arch, 416 (1990) 201-206.

[27] A.M. Gomez, B. Schwaller, H. Porzig, G. Vassort, E. Niggli, M. Egger. Increased exchange current but normal Ca^{2+} transport via Na^+-Ca^{2+} exchange during cardiac hypertrophy after myocardial infarction. Circ Res, 91 (2002) 323-330.

[28] H. Porzig, Z. Li, D.A. Nicoll, K.D. Philipson. Mapping of the cardiac sodium-calcium exchanger with monoclonal antibodies. Am J Physiol, 265 (1993) C748-756.

[29] P. Kofuji, R.W. Hadley, R.S. Kieval, W.J. Lederer, D.H. Schulze. Expression of the Na-Ca exchanger in diverse tissues: a study using the cloned human cardiac Na-Ca exchanger. Am J Physiol, 263 (1992) C1241-1249.

[30] M. Egger, A. Ruknudin, P. Lipp, P. Kofuji, W.J. Lederer, D.H. Schulze, E. Niggli. Functional expression of the human cardiac Na^{+}-Ca^{2+} exchanger in Sf9 cells: rapid and specific Ni^{2+} transport. Cell Calcium, 25 (1999) 9-17.

[31] M. Egger, E. Niggli. Paradoxical block of the Na^{+}-Ca^{2+} exchanger by extracellular protons in guinea-pig ventricular myocytes. J Physiol, 52 (2000) 353-366.

[32] M. Juhaszova, A. Ambesi, G.E. Lindenmayer, R.J. Bloch, M.P. Blaustein. Na^{+}-Ca^{2+} exchanger in arteries: identification by immunoblotting and immunofluorescence microscopy. Am J Physiol, 266 (1994) C234-242.

[33] L. Ellgaard, A. Helenius. Quality control in the endoplasmic reticulum. Nat Rev Mol Cell Biol, 4 (2003) 181-191.

[34] K. Baltensperger, H. Porzig. The P2U purinoceptor obligatorily engages the heterotrimeric G protein G16 to mobilize intracellular Ca2+ in human erythroleukemia cells. J Biol Chem, 272 (1997) 10151-10159.

[35] D.A. Ferrington, X. Chen, A.G. Krainev, E.K. Michaelis, D.J. Bigelow. Protein half-lives of calmodulin and the plasma membrane Ca-ATPase in rat brain. Biochem Biophys Res Commun, 237 (1997) 163-165.

[36] T. Iwata, C. Galli, P. Dainese, D. Guerini, E. Carafoli. The 70 kD component of the heart sarcolemmal Na^+/Ca^{2+}-exchanger preparation is the C-terminal portion of the protein. Cell Calcium, 17 (1995) 263-269.

[37] R.I. Saba, A. Bollen, A. Herchuelz. Characterization of the 70 kDa polypeptide of the Na/Ca exchanger. Biochem J, 338 (1999) 139-145.

[38] K. Takahashi, M. Azuma, J. Huschenbett, M.L. Michaelis, J. Azuma. Effects of antisense oligonucleotides to the cardiac Na^+-Ca^{2+} exchanger on calcium dynamics in cultured cardiac myocytes. Biochem Biophys Res Commun, 260 (1999) 117-121.

7. FIGURES

Figure 1: ***A*****:** Intracellular localization of a FITC-labeled AS-ODNs (identical sequence as the AS-ODNs used in the functional assays). Sf9 cells (***a***) and neonatal myocytes (***b***) were incubated with the FITC-labelled AS-ODNs (3 μM, 30 μM respectively) for 48 h in the culture medium and analyzed by confocal microscopy. ***B:*** Immunostaining of rat neonatal cardiac myocytes and binding assay with the monoclonal antibody R3F1 (3 μM) directed against the NCX: ***Ba***) NS-ODNs and ***Bb***) AS-ODNs. ***Insets*****:** Profile of fluorescence intensity distribution. In NS-ODNs-treated rat cardiac myocytes maxima of fluorescence can be observed in the plasma membrane and in cytoplasmic regions. However, the immunofluorescence approach failed to discriminate between the overall expression of the NCX1 in AS-ODNs-treated and NS-ODNs-treated rat cardiac myocytes. ***Bc***: Membrane-associated immunoreactivity in NS-and AS-ODN-treated rat cardiac myocytes (n=60); ***C***: mAb R3F1 binding curves. Control NS-ODNs and AS-ODNs-treated rat cardiac cell homogenates were equilibrated at 35°C with ^{3}H-labelled mAb R3F1 in the presence and absence of 100 μg/ml unlabeled mAb. Unspecific binding is subtracted throughout. The curves give nonlinear least-square fits to the data points. *Inset:* Maximal binding was determined in 8 experiments at 1.5-2 μg/ml mAb in the plateau range of the binding curves. After treatment with an AS-ODN directed against the NCX1 mRNA the binding affinity of the specific antibody remained unchanged.

Figure 2: ***A*** : Semi-quantitative RT-PCR to quantify NCX1 mRNA levels; ***B***: Immunodetection of the NCX1 protein expression in Sf9 cells (MOI=1, 48 h) with the monoclonal antibody R3F1. Sf9 cells with strong NCX1 immunoreactivity (***right***) as well as cells with no or very low NCX1 expression were observed in the same preparation. Approximately 60% of Sf9 cells showed positive immunostaining against the NCX1; ***C***: Maximal R3F1 binding was determined at 1.5-2 μg/ml mAb in the plateau range of the binding curves (see Fig. 1C). Experiments with Sf9 cells (native Sf9 cells, NS-ODNs and AS-ODNs treated cells) with no endogenous NCX1 under 2 conditions: high and low MOI: A more pronounced AS-ODNs effect was found under *low* MOI conditions (NS: n=6, AS: n=12, $*P<0.05$).

Figure 3: Reduced Ca^{2+} transport (influx) *via* NCX1 in AS-ODNs treated Sf9 cells expressing NCX1. ***A, B*** from left to the right: Overview confocal images of NS-ODNs (control cells, treated for 50 h, 30 μM) and AS-ODNs treated Sf9 cells (48 h, 30 μM) and the time course of $[Ca^{2+}]_i$ changes after superfusion with $[Na^+]_o$ free solution (activation of the NCX Ca^{2+} influx mode). The black bar denotes the time period of superfusion with $[Na^+]_o$ free solution; ***C:*** Ca^{2+} transport (Ca^{2+} influx) mediated by the NCX1 after 24 h (NS-ODNs: 10.31 ± 7.14 nM/s, n=25; AS-ODNs: 3.47 ± 2.4, n=8) and 48 h (NS-ODNs: 110.63 ± 7.14 nM/s, n=16; AS-ODNs: 9.9 ± 6.7, n=16; $**P < 0.01$) under control conditions (30 μM NS-ODNs) and after 30 μM AS-ODNs treatment, respectively. ***D***: Time course of repetitively activated NCX1 function (Ca^{2+} influx) by superfusion with $[Na^+]_o$ free solution in NS-ODNs pre-treated (30 μM) Sf9 cells expressing NCX1 for 24 h. The reduced second $[Ca^{2+}]_i$ peak can be explained by reduced driving force due to the loss of intracellular Na^+. MOI=1.

Figure 4: AS-ODNs significantly suppress the NCX1 function induced by flash-photolysis of caged Ca^{2+}. ***A*** and ***B*** show from top to bottom: $[Ca^{2+}]_i$ jumps induced by photorelease from 2.0 mM DM-nitrophen, the corresponding line-scan image of the fluo-3 fluorescence change and the corresponding NCX current elicited at –40 mV in 30 μM NS-ODNs (control) and 30 μM AS-ODNs treated Sf9 cells expressing NCX1; ***C:*** comparison of the Ca^{2+} transport (Ca^{2+} efflux, dCa^{2+}/dt) in control and AS-ODNs treated Sf9 cells expressing NCX1; and ***D:*** NCX1 current density. The Ca^{2+} transport as well as the exchanger current can be effectively blocked by AS-ODNs treatment of about 48 h (**$P < 0.05$ *vs* NS-ODN treated cells, n=5).

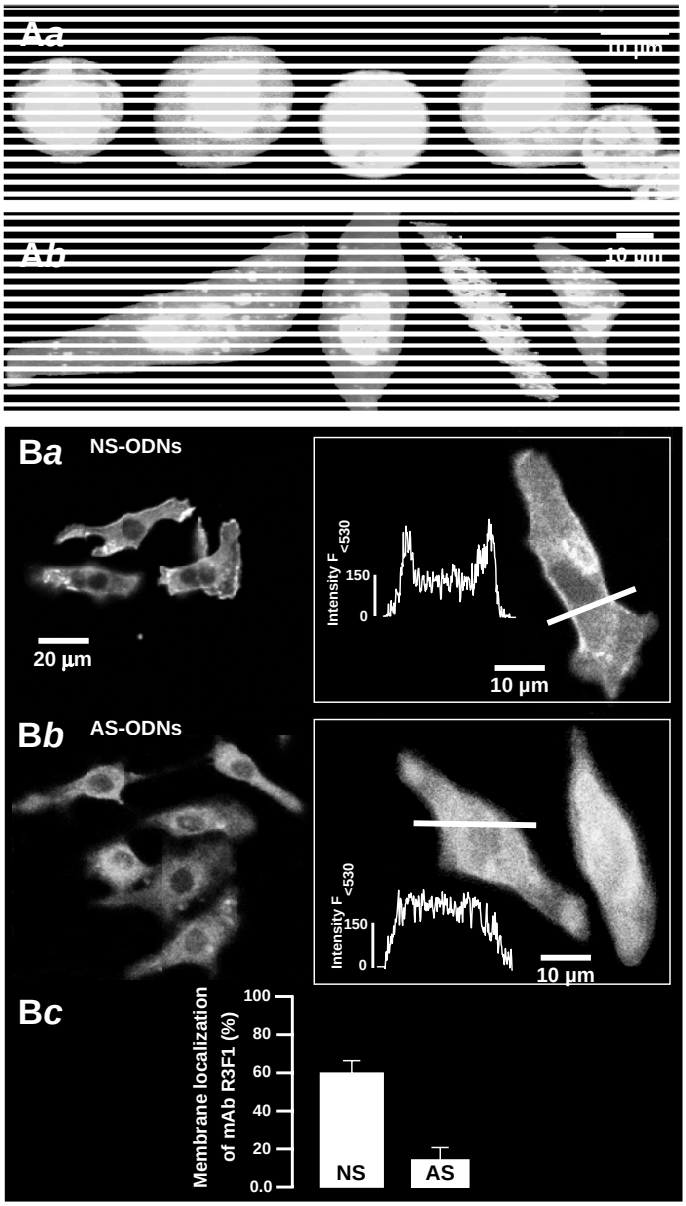
Aa
10 µm
Ab
10 µm
Ba
NS-ODNs
20 µm
Intensity F <530
150
0
10 µm
Bb
AS-ODNs
Intensity F <530
150
0
10 µm
Bc
Membrane localization of mAb R3F1 (%)
100
80
60
40
20
0.0
NS
AS
C
mAb binding (•10^3 cpm/µg protein)
35
30
25
20
15
10
5
0.0
NS
binding of mAb R3F1 (%)
100
80
60
40
20
0.0
AS
NS
0.0
0.5
1.0
1.5
2.0
2.5
3.0
mAb free (µg/ml)

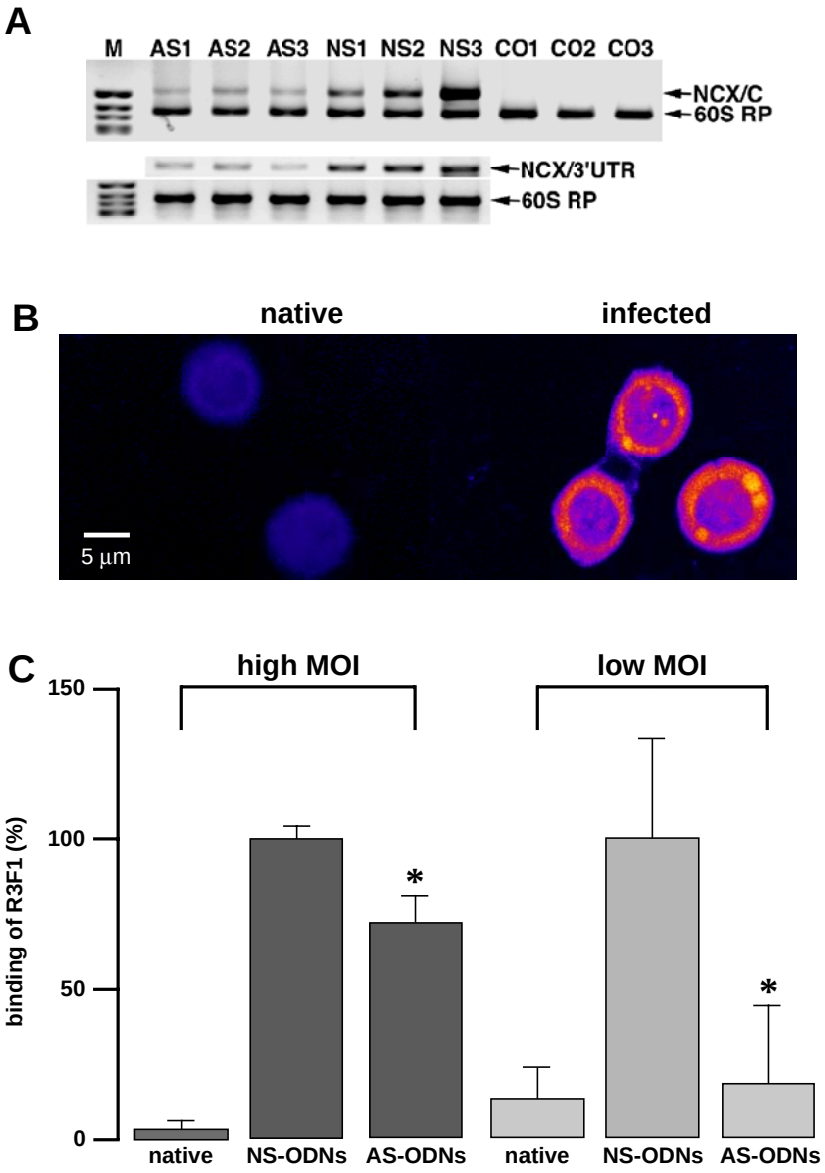
A
M
AS1
AS2
AS3
NS1
NS2
NS3
CO1
CO2
CO3
NCX/C
60S RP
NCX/3'UTR
60S RP
B
native
infected
5 µm
C
high MOI
low MOI
150
100
50
0
binding of R3F1 (%)
*
*
native
NS-ODNs
AS-ODNs
native
NS-ODNs
AS-ODNs

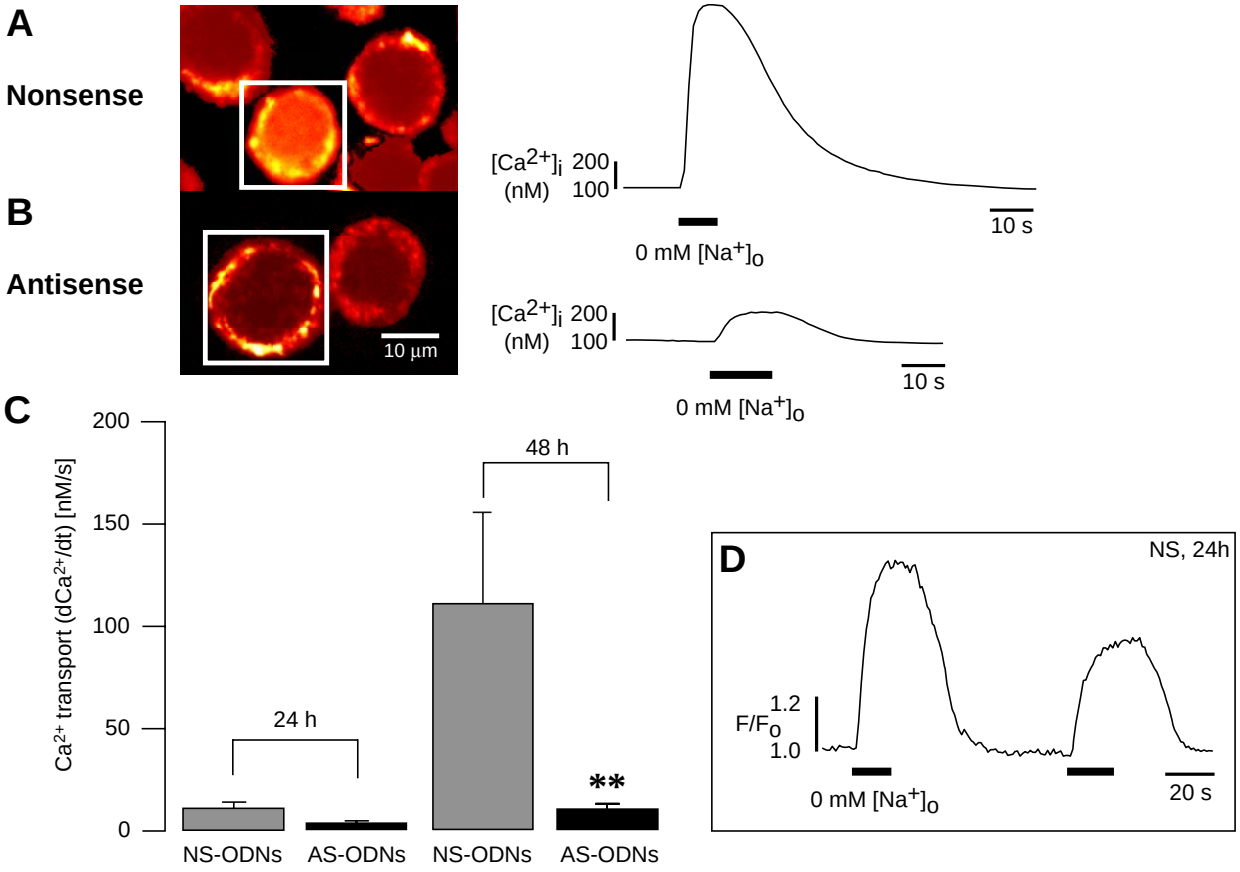
A
Nonsense
B
Antisense
10 µm
[Ca2+]i 200
(nM) 100
10 s
0 mM [Na+]o
[Ca2+]i 200
(nM) 100
10 s
0 mM [Na+]o
C
Ca2+ transport (dCa2+/dt) [nM/s]
200
150
100
50
0
24 h
48 h
**
NS-ODNs
AS-ODNs
NS-ODNs
AS-ODNs
D
NS, 24h
F/Fo
1.2
1.0
0 mM [Na+]o
20 s

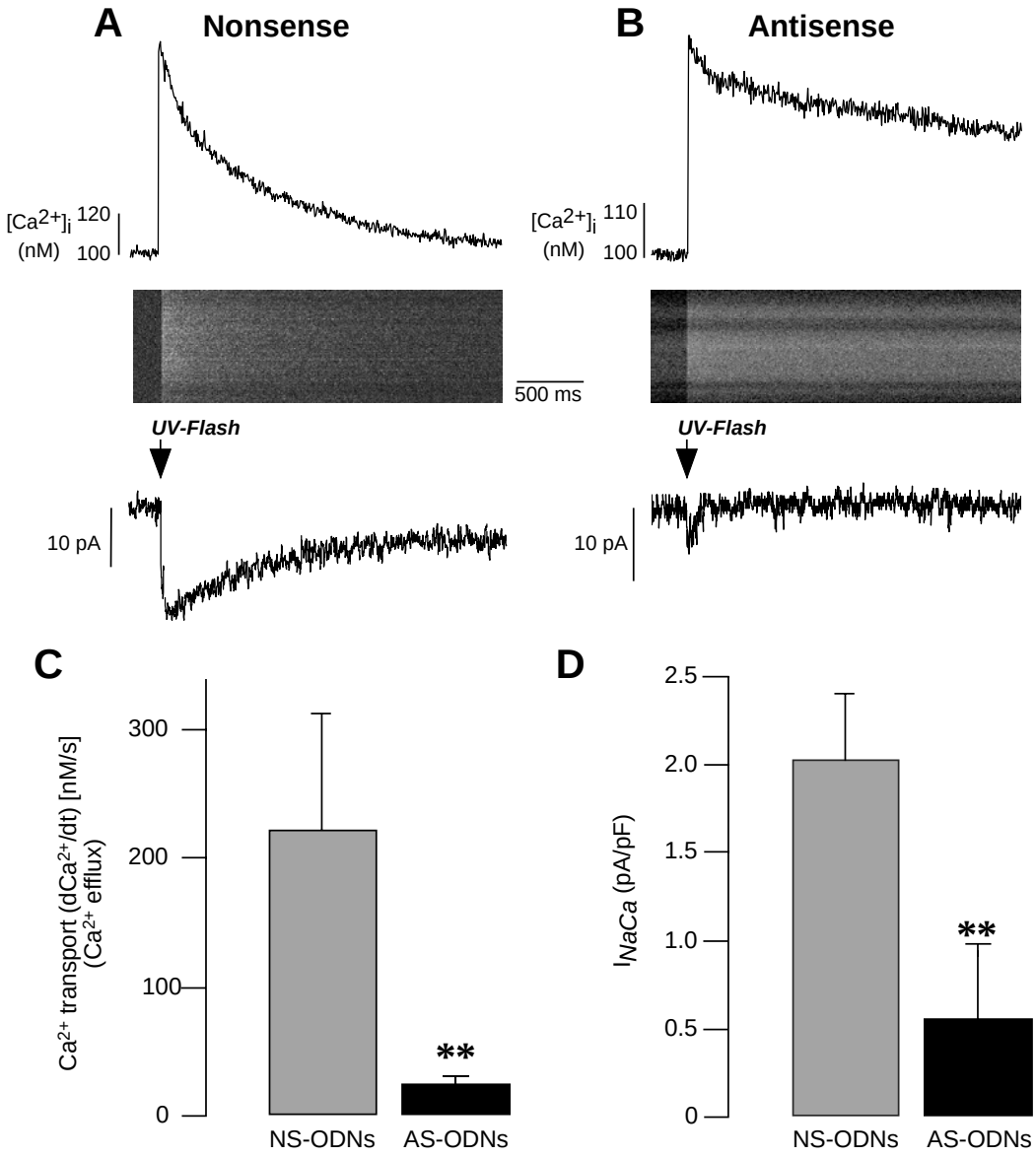
A
Nonsense
B
Antisense
[Ca2+]i 120
(nM) 100
[Ca2+]i 110
(nM) 100
500 ms
UV-Flash
UV-Flash
10 pA
10 pA
C
Ca2+ transport (dCa2+/dt) [nM/s]
(Ca2+ efflux)
300
200
100
0
**
NS-ODNs
AS-ODNs
D
INaCa (pA/pF)
2.5
2.0
1.5
1.0
0.5
0
**
NS-ODNs
AS-ODNs